

# Water productivity mapping using Landsat 8 satellite together with weather stations

Renato A. M. Franco<sup>a</sup>, Fernando B. T. Hernandez<sup>a</sup>, Antônio H. de C. Teixeira<sup>b</sup>, Janice Freitas Leivas<sup>b</sup>, Daniel Noe Coaguila<sup>a</sup>, and Christopher M. Neale<sup>c</sup>

<sup>a</sup>São Paulo State University, Ilha Solteira, Brazil

<sup>b</sup>Embrapa Satellite Monitoring, Campinas, São Paulo, Brazil

<sup>c</sup>Water for Food Global Institute at the University of Nebraska, Lincoln, USA

## ABSTRACT

The use of remote sensing satellite in conjunction with models and meteorological data enable the mapping of biophysical properties of agroecosystems with satisfactory accuracy. The main goal of this research was to determine the spatial-temporal agro-ecological indicators of water productivity in watersheds with different types of land use and occupation, using Landsat 8 images, agro-meteorological stations and application of Monteith and SAFER (Simple Algorithm for Retrieving Evapotranspiration) models to estimate the production biomass (BIO) and the actual evapotranspiration (ET), respectively. Incident global solar radiation ( $RS \downarrow$ ) is observed seasonality of radiation during the year. Higher  $RS \downarrow$  levels happen during the first and the last four months, when the Sun is around its zenith positions in the study region. During the natural dry period in the region, the  $RS \downarrow$  is lower because winter solstice time for the Southern Hemisphere, this condition it is verified the reducing in the values of ET and BIO. Average values of biophysical properties for the study period were 0.54, 0.16 and 301 K for Normalized Difference Vegetation Index, albedo and surface temperature, respectively. The highest value of BIO was 105 kg ha<sup>-1</sup>d<sup>-1</sup> and occurred in July 2013. The lowest value was 15.9 kg ha<sup>-1</sup>d<sup>-1</sup> and occurred in October 2014. ET showed a value of 1.65 mm d<sup>-1</sup> in the rainy period and 0.64 during the dry period in the study area. The highest average ET occurred in the irrigated area (June 2014), with a value of 1.89 mm d<sup>-1</sup> and a maximum of 2.46 mm d<sup>-1</sup>. WP average for the evaluated period was 3.06 Kg m<sup>-3</sup>, with the largest value of 4.91 Kg m<sup>-3</sup> in June 2013 and a minimum value of 2.45 Kg m<sup>-3</sup> in September 2013.

**Keywords:** water productivity, production biomass, evapotranspiration, SAFER

## 1. INTRODUCTION

Population growth and climate change are likely to impact upon food and water availability over the coming decades.<sup>1</sup> Human activities such as urbanization and agriculture can modify the earth's surface, altering the pattern of land use and land cover and interfering with various environmental factors.

Crop production systems are dependent on inputs and environmental services such as water, soil and climate. These activities could result, locally and regionally significant changes in the evapotranspiration, the water balance, the quantity and quality of surface and groundwater when managed improperly.

The weather is a major factor affecting agricultural production in the country and irrigated agriculture is dependent on agro-meteorological information to perform an efficient management and to provide the required amount of water to replace the hydric deficit of agricultural crops.

Irrigation in Brazil is mainly user of surface water being his primary feedstock to meet the water requirement of plants and obtaining productivity. Irrigated agriculture in Brazil uses surface water, and its primary feedstock

---

Further author information: (Send correspondence to F.B.T.H.)

F.B.T.H.: E-mail: fbthtang@agr.feis.unesp.br, Telephone: +55 18 3743 1959

R.A.M.F.: E-mail: bioramfranco@yahoo.com.br, Telephone: +55 18 3743 1959

A.H.C.T.: E-mail: heriberto.teixeira@embrapa.br, Telephone: +55 19 3211 6200

J.F.L.: E-mail: janice.leivas@embrapa.br, Telephone: +55 19 3211 6200

D.N.C.: E-mail: tuheraldo@gmail.com, Telephone: +55 18 3743 1959

to meet the water demand of plants and therefore should adopt research on efficient water use in crop production, with the development and application of tools for analysis and planning of water use.

Center pivot irrigation system is a technology used in agriculture and when they occur the increase in installed equipment numbers and its dimensions can occur an increase in water consumption of water resources. Therefore, one should adopt research efficient use of water in agricultural production, with the developing and applying tools for spatial and temporal analysis of environmental resources and the generation of data to assist in the management of water resources.

Remote sensing satellite has become an environmental analysis tool and its applications together with energy balance models associated with agro-meteorological information enables the mapping of biophysical parameters of the Earth's surface with satisfactory accuracy.

Applications of these models provide information about the estimates of the surface energy balance flows and analysis of water consumption of agro-ecosystems, especially irrigated crops and natural vegetation.<sup>2-6</sup>

Large-scale water productivity parameters obtained satellite is an important tool to support the planning of agricultural policies and decision-making about natural resources uses.<sup>7</sup> The water applied in plants provides increase in biomass of production (BIO) and evapotranspiration (ET).<sup>3,4,7</sup> These agroecological indicative to assess the water of productivity in agricultural and environmental systems.

BIO is related to the Photosynthetically Active Radiation (PAR), which is part of the solar radiation short-wave absorbed by chlorophyll in photosynthesis and energy PAR uses only 40% to 50% of the total energy of solar radiation. PAR is thus a fraction of the incoming solar radiation ( $RS \downarrow$ ). PAR refers to the visible part of the solar spectrum between 0.4 and 0.7  $\mu\text{m}$ , where chlorophyll absorbs solar radiation.

The quantification of large-scale BIO allows comparisons between crops different, promoting spatial and temporal information and your estimate is based on the ( $RS \downarrow$ ). The model was developed by Monteith<sup>8</sup> and is based on the light-use efficiency concept (LUE), this technique associated with the parameters obtained by orbital data are acceptable.<sup>2,7-9</sup> LUE is defined as the capacity of the vegetation to use gross primary productivity per unit of Absorbed Photosynthetically Active Radiation (APAR) that is limited by temperature and water scarcity.<sup>10,11</sup> The model was applied in the Brazilian semi-arid region, in the basin of the São Francisco River and achieved satisfactory results in the study.<sup>2,7</sup>

Water productivity (WP) may be defined as the ratio of the net benefits from crop, forestry, fishery, livestock and mixed agricultural systems to the amount of water required to produce those benefits.<sup>7,12</sup> According to authors considering the vegetation, WP may be the BIO by the water consumed by the vegetated surface, including water originated precipitation, irrigation, flow and variations soil moisture.

Water productivity is dependent on evapotranspiration and its quantification is determined by the algorithm SAFER (Simple Algorithm for Retrieving Evapotranspiration) allows to estimate ET by Penman Monteith equation in conjunction with data biophysical parameters generated by remote sensing using.<sup>5,6</sup>

For tropical Brazilian condition, developed and validated two algorithms with different data field hydrological conditions involving natural vegetation and agricultural ecosystems with different types of cultures to determine the ET-based Penman-Monteith.<sup>5</sup>

The first model uses meteorological measurements and estimates of the net radiation ( $R_n$ ), the heat flow in the ground ( $G$ ) and the aerodynamic resistance ( $R_a$ ) and surface area ( $RS \downarrow$ ) to the water vapor flux associated with data obtained by remote sensing. The second is based on surface albedo data ( $\alpha_b$ ), surface temperature ( $T_0$ ) and NDVI (Normalized Difference Vegetation Index). For both it used evapotranspiration data reference (ET) calculated with data from meteorological stations to determine the instantaneous values of the ratio  $ET/ET_0$  in conjunction with satellite data.<sup>5</sup> The second model came to be known as SAFER (Simple Algorithm For Retrieving Evapotranspiration) and has the advantage of not using classification information crop nor extreme dry conditions.<sup>6,7</sup>

SAFER is an ET monitoring system using remote sensing, has the advantage of simplicity of application, the absence of the need of neither crop classification nor extreme conditions.<sup>6</sup> The SAFER algorithm has the

additional advantage of the possibility for using daily weather data from either conventional or automatic agrometeorological station.<sup>13</sup> A description of SAFER and an application for monitoring large-scale evapotranspiration were reported by Teixeira *et al.*<sup>5,13</sup>

The objective of this study is to determine the spatial-temporal agro-ecological indicators of water productivity in watersheds with different types of land use and occupation, using Landsat 8 images, weather stations and application of Monteith and SAFER models to estimate the BIO and the ET, respectively. In this connection, the concepts of water productivity are useful for efficient planning and decision-making at farmer level, for integrating information from many sources, and for generating new information. Agro-ecological indicators are going support in the management of water resources in Northwestern of São Paulo State.

## 2. MATERIAL AND METHODS

### 2.1 The study area and data acquisition

Figure 1 shows the locations of municipalities in the Northwestern of São Paulo State, together with the weather station stations used for interpolation processes inside study area. Interpolation method was moving surface, which requires a point meteorological map as input and returns a raster map as output. The meteorological variables are interpolated into daily maps at 30-m resolution by the moving surface method. After, the raster map will be included in the modeling of water productivity.

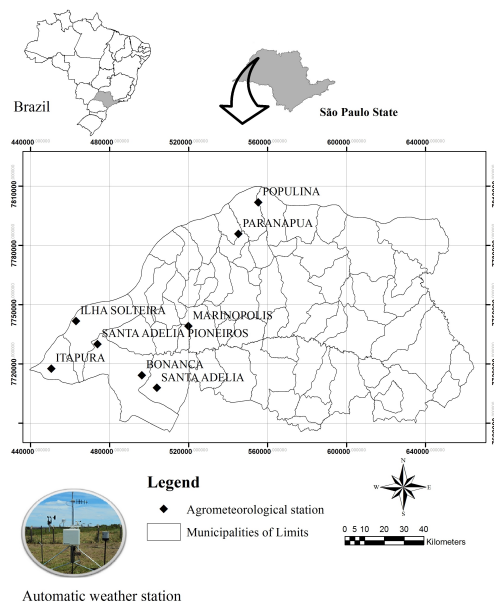


Figure 1. Study areas location in the Northwestern of São Paulo State, together with the weather station.

Weather data processing comprises daily data, including average air temperature ( $T_a$ ), reference evapotranspiration ( $ET_0$ ) based on the Penman-Monteith equation,<sup>14</sup>  $RS \downarrow$  is measured by pyranometer and accumulated precipitation ( $P$ ), are collected from the UNESP.<sup>15</sup>

Weather data were analyzed together with the image data during the study period, with the purpose of influence of climatic conditions. In the Bonança meteorological station (Figure 1), the average annual air temperature is 24.2 °C. Average annual daily temperatures range from 14.7 °C to 36.7 °C. Mean annual precipitation is about 1.208 mm and accumulated reference evapotranspiration is 1.413 mm. Although, the regional climate is classified as savanna - Cwa,<sup>16</sup> there exists difference in precipitation pattern. Highest accumulated rainfall occurs in summer (December, January, and February) and reduction in winter period (June, July and August).

In the water balance study area from 2000 to 2010 was an average annual rainfall of 1,354 mm and the average annual evaporation of 1,506 mm. Characterized by presenting seven months with water deficit (April to October) with the annual total of 442 mm and 296 mm of excess water in January, February and March.<sup>15</sup>

Figure 2 show location of the research area. Study area comprising a surface involving three adjacent watersheds with different types of land use and occupation. The watershed was carried out in the Tietê river basin, which is located in the Northwestern of São Paulo State.

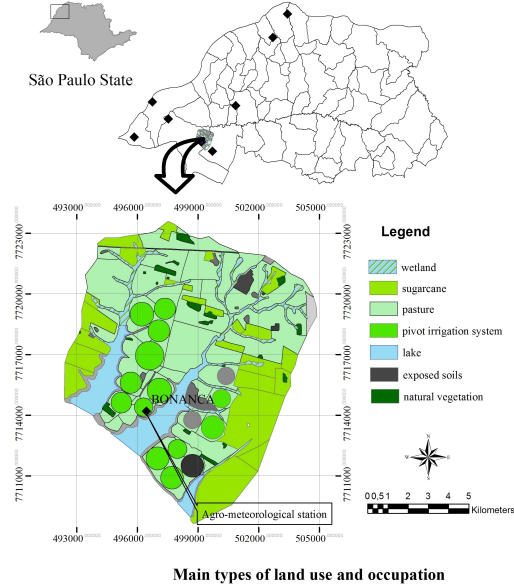


Figure 2. Land cover map of study area obtained by multispectral classification of OLI image (Landsat-8 OLI at 01 Jun 2013).

The Landsat 8 satellite images the entire Earth every 16 day. Landsat 8 carries two instrument, the Operational Land Imager (OLI) sensor and the Thermal Infrared Sensor (TIRS) sensor provides two thermal bands. ( $T_0$ ) data from the TIRS onboard Landsat 8 satellite were used in this study.

The Landsat 8 satellite images used in this study were available from the United States Geological Survey (USGS) and Earth Resource Observation and Science EROS.<sup>17</sup> Landsat images of Path 222/Row 074 were considered for the study area. Obtained of the cloud-free satellite image dates, the following year and Julian days (DOY: Day of Year): 2013/152; 2013/185; 2013/217; 2013/249; 2013/313; 2014/28; 2014/76; 2014/92; 2014/124; 2014/172; 2014/204; 2014/220; 2014/252; 2014/284. Resulting 14 satellite images at different months of the years, with 5 being for 2013 and 9 for 2014.

## 2.2 Remote sensed parameters

The spectral radiances ( $L_\lambda$ ) ( $W m^{-2} sr^{-1} m^{-1}$ ), were computed from Digital Number (DN):

$$L_\lambda = GAIN * DN + Offset, \quad (1)$$

where Gain and Offset refer to the values given in the metadata file.<sup>18</sup>

The planetary albedo for each Landsat 8 satellite band ( $\alpha_{pb}$ ) was calculated as:

$$\alpha_{pb} = \frac{L_\lambda \pi d^{-2}}{Ra_b \cos \varphi}, \quad (2)$$

where  $L_\lambda$  is the spectral radiance for the images spectral bands ( $W m^{-2} sr^{-1} m^{-1}$ ), utilizing band 2 to 7 (Band 2: 0.45 - 0.51  $\mu m$ ; Band 3: 0.53 - 0.59  $\mu m$ ; Band 4: 0.64 - 0.67  $\mu m$ ; Band 5: 0.85 - 0.88  $\mu m$ ; Band 6: 1.57 -

1.65  $\mu\text{m}$ ; Band 7: 2.11 - 2.29  $\mu\text{m}$ );  $d^{-2}$  is the relative earth-sun distance;  $Ra_b$  is the mean solar irradiance at the top of the atmosphere (or atmospheric irradiance) for each band ( $\text{W m}^{-2} \mu\text{m}^{-1}$ ) and  $\varphi$  the solar zenith angle.<sup>19</sup>

For each band was obtained  $Ra_b$ , expressed from the Plancks Law. The weights of each band to calculate the integral of the spectral radiation in the wavelength interval and considering its fraction over the solar spectrum, assuming the sun as a blackbody. Then, the broadband planetary albedo ( $\alpha_a$ ) was calculated as the total sum of the different narrow-band  $\alpha_{pb}$  values according to the weights for each band ( $w_b$ ).<sup>20</sup>

$$\alpha_p = \sum w_b \alpha_{pb}, \quad (3)$$

where the  $w_b$  values were computed as the ratio of the amount of the incoming shortwave radiation from the sun at the top of the atmosphere in a particular band and the sum for all the bands.<sup>20</sup>

### 2.3 Simple Algorithm for Retrieving Evapotranspiration - SAFER

SAFER is a model that requires biophysical parameters obtained by remote sensing together with data from meteorological stations. The remote sensing parameters involved in NDVI (Normalized Difference Vegetation Index), surface albedo ( $\alpha_0$ ), surface temperature ( $T_0$ ) were determined and added in the Equation below:<sup>5,6,19</sup>

$$\frac{ET}{ET_0} = \exp \left[ a + b \left( \frac{T_0}{\alpha_{0NDVI}} \right) \right], \quad (4)$$

where a and b are regression coefficients.<sup>5</sup> For this study adopted value 1.0 for the a and -0.008 for the b coefficients of the Equation 4.<sup>19</sup> The  $ET_0$  was obtained in an automatic station and added in Equation 4.  $NDVI = (\alpha_{NIR} - \alpha_{RED}) / (\alpha_{NIR} + \alpha_{RED})$  and  $\alpha_{NIR}$  and  $\alpha_{RED}$  are the near-infrared and infrared band reflectivity, respectively.

### 2.4 Net Radiation

The daily (24-hour) values of ( $R_n$ ) were determined according to Equation 5:<sup>3,4</sup>

$$R_n = (1 - \alpha_0)RS \downarrow - a\tau_{sw} \quad (5)$$

where  $RS \downarrow$  is solar radiation in  $\text{MJ m}^{-2} \text{d}^{-1}$ , obtained in the weather station; a is the regression coefficient of the relationship between net long wave radiation and atmospheric transmissivity ( $\tau_{sw}$ ) at the daily scale, according to the following Equation 6:

$$a_1 = bT_a - c \quad (6)$$

where b and c - are regression coefficients and show the following values, 6.99 and 39.93, respectively.<sup>2</sup> $T_0$  are measurements obtained at weather station (Figure 3), interpolation method included in the Equation 6.

### 2.5 Photosynthetically Active Radiation - PAR

It's the part of the short wave solar radiation (0.3 to 3.0  $\mu\text{m}$ ) that supports photosynthesis in green plants and varies between 0.45 and 0.5 of the solar radiation.<sup>21</sup> The daily values of  $RS \downarrow$  for each DOY were used to estimate the values of PAR ( $\text{W m}^{-2}$ ) for the same time scale (24 hours). PAR is calculated following the formulation:

$$PAR = aRS \downarrow \quad (7)$$

where a=0.44 is the constant of the regression equation found under the Brazilian semiarid conditions that reflects the portion of  $RS \downarrow$  that can be used by leaf chlorophyll for photosynthesis.<sup>3,4</sup>

It was estimated from the Equation 8 by obtaining the Absorbed Photosynthetically Active Radiation (APAR) ( $\text{W m}^{-2}$ ):

$$APAR = fPAR \quad (8)$$

The factor  $f$  was estimated from the NDVI values. Where the values of  $a$  and  $b$  are 1.257, -0.161, respectively.<sup>8</sup>

## 2.6 Production biomass - BIO

BIO is computed as:

$$BIO = \varepsilon_{max} E_f APAR \cdot 0.864 \quad (9)$$

where  $E_f$  (evaporative fraction) is the ratio of the latent heat flux ( $\lambda E$ ) to  $R_n$ .  $E_f$  is strongly linked to the vegetation water status [5], being  $\lambda E$  acquired by transforming ET into energy units;  $\varepsilon_{max} E_f$  is the maximum light use efficiency, which was considered  $2.5 \text{ g MJ}^{-1}$  for the majority of c4 species in the studied area; and 0.864 is a unit conversion factor.<sup>2,19</sup>

## 2.7 Water productivity - WP

For water productivity (WP) analysis, involving the watershed, the following equation was used:<sup>2</sup>

$$PA = \frac{BIO}{ET} \quad (10)$$

where BIO was obtained from the Equation 9 and ET was acquired in Equation<sup>7</sup>

## 3. RESULTS AND DISCUSSION

### 3.1 Agrometeorological parameters

As the agro-meteorological parameters main factors drive for water flux and vegetation development are solar radiation and precipitation.<sup>7</sup> The monthly analysis of the solar radiation and precipitation is presented in Figure 3, during the study reference year of 2013 and 2014.  $RS \downarrow$  is observed seasonality of radiation during the year.

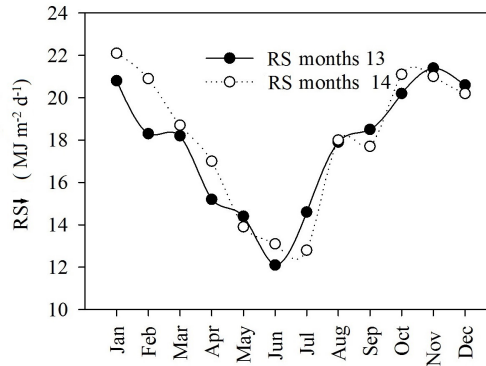


Figure 3. Monthly average daily values of  $RS \downarrow$ .

Higher  $RS \downarrow$  levels happen during the first and the last four months (Sep, Oct, Nov and Dec), when the Sun is around its zenith positions in the study region. During the naturally dry period in the region, the  $RS \downarrow$  is lower because winter solstice time for the South hemisphere, this condition it is verified the reducing in the values of ET and BIO. On the other hand, during the rainy period there high values of BIO and ET.

Analyzing the years 2013 and 2014, the amounts of annual precipitation in 2013 was 1,066.4 mm and for the year 2014 was 1,174.3 mm. Figure 4 presents the monthly-cumulated precipitation of year 2013 and 2014. Monthly accumulated precipitation for the years 2013 and 2014 verified was an increase in the rainy period and the reduction from the dry period. Jun (2013) and July (2014) with rainfall above 50 mm, atypical condition

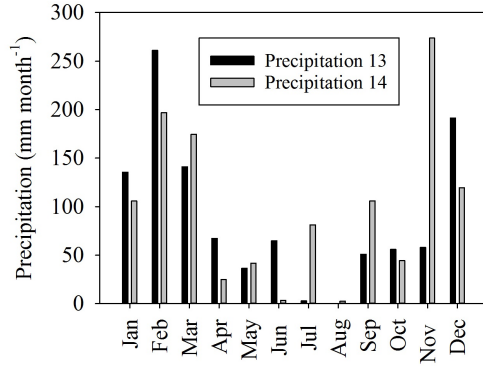


Figure 4. Monthly totals of precipitation.

for period of the year. According to the technical report of the CPTEC the month of June 2013 the Southeast region of Brazil showed rainfall above the climatological values,<sup>22</sup> a similar situation was found in the survey by agro-meteorological station network.<sup>15</sup>

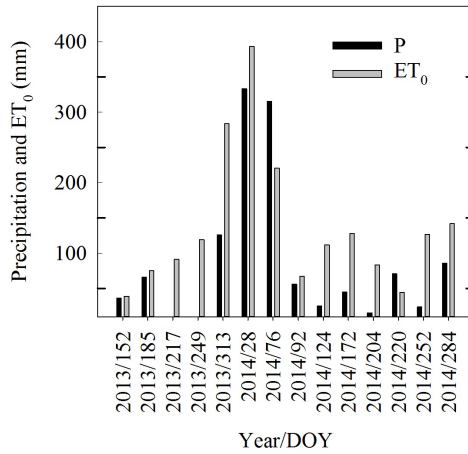


Figure 5. P accumulated and ET<sub>0</sub> accumulated between the days of the years.

Figure 5 the cumulative rainfall between the years and DOY day for each evaluated image. The months of August (DOY: 217) and September (DOY: 249) 2013 were with values below 10 mm of accumulated rainfall. In relation to ET<sub>0</sub> accumulated, one can see the concentration of the highest values from November to March.

### 3.2 Biophysical parameters

Figure 6 represents spatial-temporal of the NDVI values and the average for each year/DOY of the assessed watersheds. The largest values happened during the rainy season and reduced values in the dry season. The average study period was 0.44, the lowest mean value was 0.36 (SD: ±0.19) and occurred in 2014/252. The highest value occurred in 2014/28, with an average value of 0.54 (SD: ±0.26). Precipitation affects the values of NDVI (Figure 6); in that condition, higher values of NDVI indicate greater vigour and amounts of vegetation.

In irrigated areas, high NDVI values were found, with 0.69. Other class of land cover which presented high NDVI values were a natural vegetation, citrus, pasture, with values of 0.46, 0.45 and 0.43, respectively. Irrigated harvesting area was observed reduction in NDVI values. On the other hand, in the vegetation developmental condition is observed high values of NDVI.

Average value of the  $\alpha_0$  for the period assessed among 2013-2014 was 0.16. Highest values occurred in the DOY/Year 185/2013 (Jul), 252/2013 (Sep) and 284/2013 (Oct), with values of 0.22 (SD:±0.01), 0.19 (SD:±0.02),

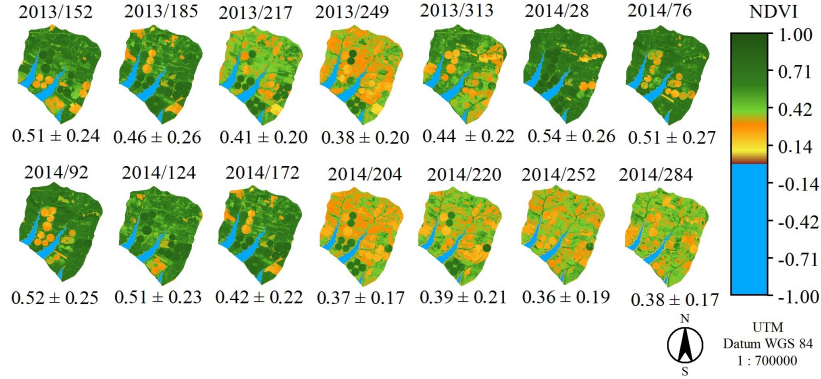


Figure 6. Spatio-temporal distribution of the value of the NDVI for the watersheds during the years from 2013 to 2014, for every day of the year (DOY), average NDVI and SD value.

0.19 (SD:±0.01), respectively. The lower values correspond to pixels where moisture conditions dominant, due to rainy season (Figure 5).

Other studies cited,  $\alpha_0$  also depends on moisture conditions.<sup>6,13,23–25</sup> In irrigated area, as the vegetation canopy fraction decreases, surface albedo gradually increases. The albedo values of vegetation cover areas significantly less than the non-coverage areas, the smallest is lakes.

There was more precipitation in January, February and April, and precipitation significantly reduced the surface albedo (Figure 3 and 7). On the other hand, increase in the  $\alpha_0$  values with decreasing precipitation.

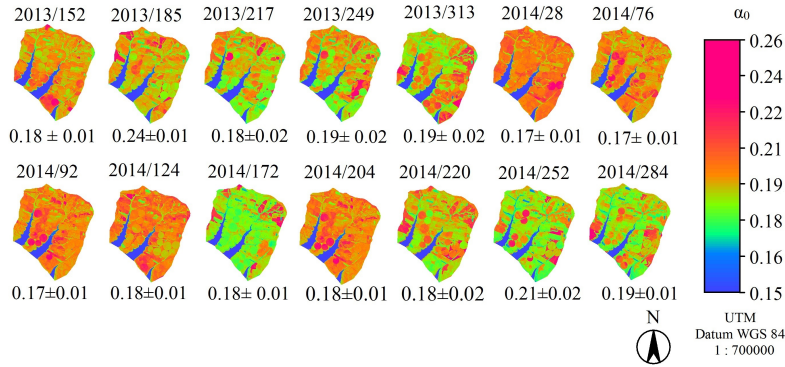


Figure 7. Spatio-temporal distribution of the value of the  $\alpha_0$  for the watersheds during the years from 2013 to 2014, for every day of the year (DOY), average  $\alpha_0$  and SD value.

The surface temperature distribution can be clearly seen from Figure 8. In the study of area, most of the water temperature between 297 K to 299 K. Area irrigated by center pivot shows values between 289 K - 295 K (DOY:172), while the bare soil temperatures were higher than 313 K (DOY:284). Use sugar cane has low values of surface temperature, observed in image (DOY:92). The result are consistent with those obtained in Nilo Coelho irrigation scheme (Brazil) with the same method, where  $T_0$  varies between 295.5 K and 315.5 K.<sup>6</sup>

### 3.3 Temporal-spatial Variability Analysis of ET by SAFER

Figure 9 shows the image illustrating the temporal-spatial variations of the ET derived by the SAFER procedures. The highest ET occurred in water-bodies and vegetated areas. The lowest ET value appeared in termo-hydrological unfavourable conditions throughout the year. It appears that the SAFER was able to capture the combined effects of meteorology, soil, and vegetation on spatial-temporal patterns of ET distribution.



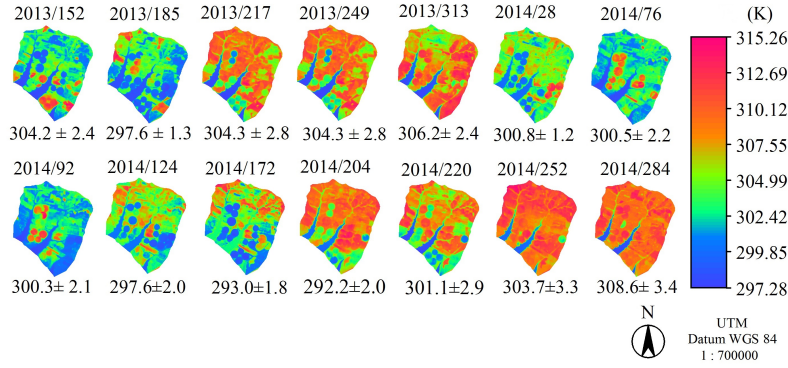


Figure 8. Spatio-temporal distribution of the value of the  $T_0$  for the watersheds during the years from 2013 to 2014, for every day of the year (DOY), average  $T_0$  and SD value.

The daily ET shows the significant spatial variations, ranging from less than 0.52 mm in developed areas to 6.00 mm in water-bodies such a lake or river, with the daily mean ET of 1,18 mm for the whole study area (from 2013 to 2014). The areas with higher mean daily ET are lakes and vegetated areas and the mean ET in these areas ranges from 1.7 to 2.5 mm  $d^{-1}$ .

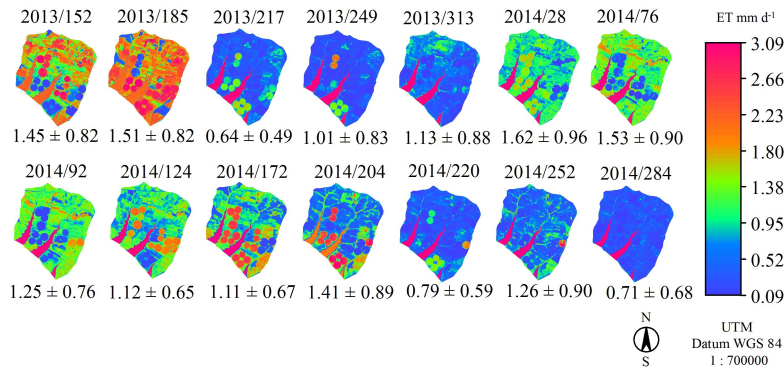


Figure 9. Spatio-temporal distribution of the value of the ET for the watersheds during the years from 2013 to 2014, for every day of the year (DOY), average ET and SD value.

### 3.4 Spatial and Temporal Distribution of Biomass

Figure 10 shows the spatial distributions of daily values of BIO from 2013 to 2014 for DOY, average and standard deviation (SD). Analysing only irrigated crops, in 2013 (DJ: 185) the are irrigated by center pivots presented in average 106.1 kg  $ha^{-1}d^{-1}$  (SD:±59.0) and in 2014 (DOY:28) it was 129.43 kg  $ha^{-1}d^{-1}$  (SD:±21.6),with maximum value of 159.29 kg  $ha^{-1}d^{-1}$ . In June 2014 (DOY: 172), the maximum value was 125.2 kg  $ha^{-1}d^{-1}$  and an average of 43.6 (SD:± 64.2). In the semi-arid region of Brazil, lower values for BIO have been found between the months of July and September, and high values occurred in the rainy season which span from the period of February to April.<sup>7</sup>

In the Northwestern São Paulo State, the image of March (2004/80) showed high value of BIO due to the rainy season in the region. In the dry season there is a reduction in the value of BIO in watershed, the values of BIO are high in irrigated areas due to the daily irrigation center pivots.<sup>26</sup> The conditions observed in Franco et al.,<sup>26</sup> are also observed in the period between 2013 and 2014, with reductions in BIO values in the dry season in the region.

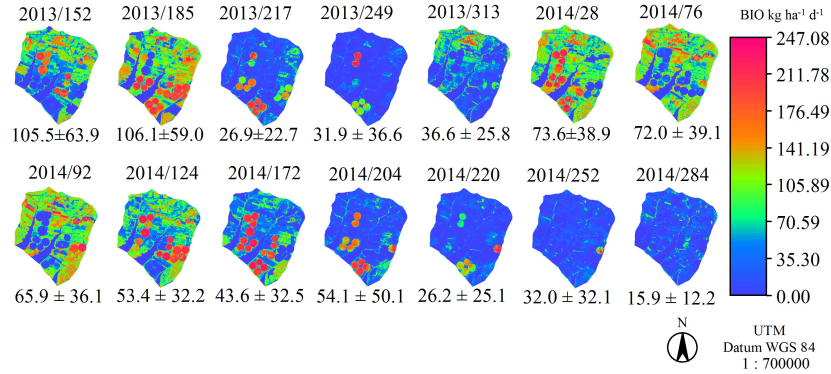


Figure 10. Spatio-temporal distribution of the value of the BIO for the watersheds during the years from 2013 to 2014, for every day of the year (DOY), average BIO and SD value.

### 3.5 Spatial and Temporal Distribution of Water Productivity

The maximum WP means value occurred in June/2013 (DOY:152), with 4,91 Kg m<sup>-3</sup> (SD:±1.89), the second highest value was in 2013 (June/DOY:185), with a means value of 3,90 kg m<sup>-3</sup> (SD:±1.80) (Figure 11). Irrigated agriculture show the highest WP value in 2013 (DOY:152), with maximum value of 8.20 kg m<sup>-3</sup> and mean value of 6.98 kg m<sup>-3</sup> (SD:±2.0).

The lowest WP was obtained by images of DOY 249 (September, 2013) and 284 (October, 2014), because of the dry season with low soil moisture conditions. ET<sub>0</sub> accumulated higher than the volume of accumulated rainfall between DOY analysed (Figure 5).<sup>15</sup>

Assessing the WP for different types of land use, verified mean value of 4.82 Kg m<sup>-3</sup> for the sugarcane not irrigated in 2013 (June), at the same date occurred a mean value of 6.34 Kg m<sup>-3</sup> for natural vegetation. In 2001 the average value for natural vegetation was 3.4 Kg m<sup>-3</sup> and sugarcane reached a maximum value of 5.0 Kg m<sup>-3</sup>, and mean 3.0 Kg m<sup>-3</sup>.<sup>26</sup> Teixeira et al.<sup>7</sup> reported that the WP higher than 4.5 Kg m<sup>-3</sup> including both, irrigation and natural conditions in the mixed Brazilian semi-arid, along the year of 2011.

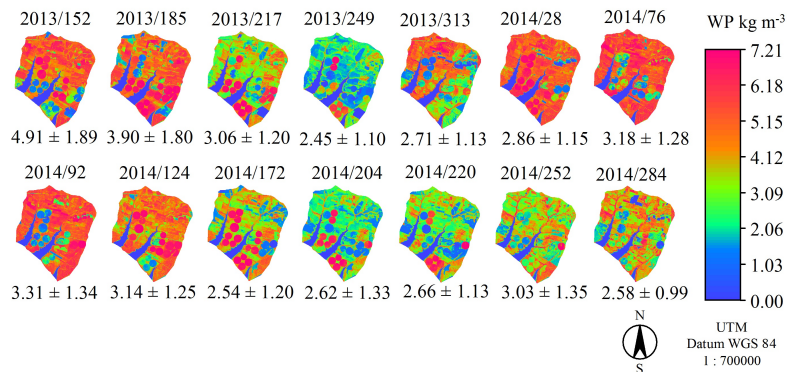


Figure 11. Spatio-temporal distribution of the value of the WP for the watersheds during the years from 2013 to 2014, for every day of the year (DOY), average WP and SD value.

## 4. CONCLUSIONS

The main results of this work have demonstrated that the satellite-based agro-meteorological station was able to appropriately estimate the productivity water.

Studies have shown that the albedo is sensitive to the distribution of precipitation pattern in typical agro-ecosystem in study area.

Combination remote sensing parameters from Landsat 8 satellite images and weather data from agro-meteorological stations allowed the water productivity assessment in watersheds along the years of 2013 to 2014.

SAFER model was efficient for the study and to identification of the termo-hydrological conditions of the imagens evaluated in the dry and rainy seasons. The SAFER model used in this study were applied reasonably quickly because of their extensive validations during many other studies and the availability of existing datasets.

WP values were higher in the irrigated, mainly in the crop production and reduction during the fallow period, represent by pixel reddish.

## ACKNOWLEDGMENTS

FAPESP and CNPq, are acknowledged for the financial support for the projects.

## REFERENCES

- [1] Wiltshire, A. J., Kay, G., Gornall, J., and Betts, A. R., “The impact of climate, co2 and population on regional food and water resources in the 2050s,” *Sustainability* **5**, 2129–2151 (2013).
- [2] Teixeira, A. d. C. and Bassoi, L. H., “Crop water productivity in semi-arid regions: From field to large scales,” *Ann. Arid Zone* **48**, 1–13 (2009).
- [3] Teixeira, A. H. C., Bastiaanssen, W. G. M., Ahmad, M., and Bos, M., “Reviewing sebal input parameters for assessing evapotranspiration and water productivity for the low-middle são francisco river basin, brazil: Part a: Calibration and validation,” *Agricultural and Forest Meteorology* **149**(3), 462–476 (2009).
- [4] Teixeira, A. H. C., Bastiaanssen, W. G. M., Ahmad, M., and Bos, M., “Reviewing sebal input parameters for assessing evapotranspiration and water productivity for the low-middle são francisco river basin, brazil: Part b: Application to the regional scale,” *Agricultural and Forest Meteorology* **149**(3-4), 477–490 (2009).
- [5] Teixeira, A. H. C., “Determining regional actual evapotranspiration of irrigated crops and natural vegetation in the são francisco river basin (brazil) using remote sensing and penman-monteith equation,” *Remote Sensing* **2**(5), 1287–1319 (2010).
- [6] Teixeira, A. H., Hernandez, F. B., and Lopes, H. L., “Application of landsat images for quantifying the energy balance under conditions of land use changes in the semi-arid region of brazil,” in [*SPIE Remote Sensing*], 85310P–85310P, International Society for Optics and Photonics (2012).
- [7] Teixeira, A. H., Scherer-Warren, M., Hernandez, F. B., Andrade, R. G., and Leivas, J. F., “Large-scale water productivity assessments with modis images in a changing semi-arid environment: A brazilian case study,” *Remote Sensing* **5**(11), 5783 (2013).
- [8] Bastiaanssen, W. G. and Ali, S., “A new crop yield forecasting model based on satellite measurements applied across the indus basin, pakistan,” *Agriculture, ecosystems & environment* **94**(3), 321–340 (2003).
- [9] Zwart, S. J., Bastiaanssen, W. G., de Fraiture, C., and Molden, D. J., “Watpro: A remote sensing based model for mapping water productivity of wheat,” *Agricultural Water Management* **97**(10), 1628–1636 (2010).
- [10] Running, S. W., Nemani, R. R., Heinsch, F. A., Zhao, M., Reeves, M., and Hashimoto, H., “A continuous satellite-derived measure of global terrestrial primary production,” *Bioscience* **54**(6), 547–560 (2004).
- [11] Landsberg, J. J. and Sands, P., [*Physiological ecology of forest production: principles, processes and models*], vol. 4, Academic Press (2010).
- [12] Molden, D., Bin, D., Loeve, R., Barker, R., and Tuong, T., “Agricultural water productivity and savings: policy lessons from two diverse sites in china,” *Water Policy* **9**(S1), 29–44 (2007).
- [13] Teixeira, A. H. d. C., Hernandez, F. B., Andrade, R. G., Leivas, J. F., and Bolfe, E. L., “Energy balance with landsat images in irrigated central pivots with corn crop in the são paulo state, brazil,” in [*SPIE Remote Sensing*], 92390O–92390O, International Society for Optics and Photonics (2014).
- [14] Allen, R. G., Pereira, L. S., Raes, D., Smith, M., et al., “Crop evapotranspiration-guidelines for computing crop water requirements-fao irrigation and drainage paper 56,” *FAO, Rome* **300**(9), D05109 (1998).

- [15] UNESP, “Access to daily data: Bonança - municipality of Pereira Barreto, SP.” 26 February 2016 <https://clima.feis.unesp.br>. (Accessed: 15 September 2015).
- [16] Peel, M. C., Finlayson, B. L., and McMahon, T. A., “Updated world map of the köppen-geiger climate classification,” *Hydrology and Earth System Sciences Discussions Discussions* **4**(2), 439–473 (2007).
- [17] USGS, “Earth resource observation and science–eros.” 15 February 2015 <http://glovis.usgs.gov/> (2015).
- [18] Vanhellemont, Q. and Ruddick, K., “Turbid wakes associated with offshore wind turbines observed with landsat 8,” *Remote Sensing of Environment* **145**, 105–115 (2014).
- [19] Teixeira, A. H. d. C., Hernandez, F. B. T., Lopes, H., Scherer-Warren, M., and Bassoi, L. H., [*Remote Sensing of Energy Fluxes and Soil Moisture Content*], vol. 1, ch. A comparative study of techniques for modelling the spatiotemporal distribution of heat and moisture fluxes in different agro-ecosystems in Brazil, 165–187, CRC Press:, Boca Raton, Florida, 1 ed. (2014).
- [20] Teixeira, A. H. d. C., Leivas, J. F., Andrade, R. G., Hernandez, F. B., and Franco, R., “Modelling radiation and energy balances with landsat 8 images under different thermohydrological conditions in the brazilian semi-arid region,” in [*SPIE Remote Sensing*], 96370U–96370U, International Society for Optics and Photonics (2015).
- [21] Jacovides, C., Tymvios, F., Asimakopoulos, D., Theofilou, K., and Pashiardes, S., “Global photosynthetically active radiation and its relationship with global solar radiation in the eastern mediterranean basin,” *Theoretical and Applied Climatology* **74**(3-4), 227–233 (2003).
- [22] CPTEC, “Technical report:Climanlise - Monitoring Bulletin and climate analysis - CPTEC-INPE.” 26 February 2016 <http://climanalise.cptec.inpe.br/~rclimanl/boletim/> (2015). (Accessed: 15 September 2015).
- [23] Li, S.-G., Eugster, W., Asanuma, J., Kotani, A., Davaa, G., Oyunbaatar, D., and Sugita, M., “Energy partitioning and its biophysical controls above a grazing steppe in central mongolia,” *Agricultural and Forest Meteorology* **137**(1), 89–106 (2006).
- [24] van Dijk, A. I., Bruijnzeel, L. S., and Schellekens, J., “Micrometeorology and water use of mixed crops in upland west java, indonesia,” *Agricultural and forest meteorology* **124**(1), 31–49 (2004).
- [25] Teixeira, A., Bastiaanssen, W., Ahmad, M.-u.-D., Moura, M. d., and Bos, M., “Analysis of energy fluxes and vegetation-atmosphere parameters in irrigated and natural ecosystems of semi-arid brazil,” *Journal of Hydrology* **362**(1), 110–127 (2008).
- [26] Franco, R., Hernandez, F. B., and Teixeira, A. H., “Water productivity of different land uses in watersheds assessed from satellite imagery landsat 5 thematic mapper,” in [*SPIE Remote Sensing*], 92392E–1– 92392E–7, International Society for Optics and Photonics (2014).